Lu, X.; Soomere, T.; Stanev, E.V.; Murawski, J.:

**Identification of the environmentally safe fairway in the South-Western Baltic Sea and Kattegat**

In: Ocean Dynamics (2012) Springer

DOI: 10.1007/s10236-012-0532-x

# Event driven approach for the identification of the environmentally safe fairway in the south-western Baltic Sea and Kattegat

Xi Lu[1], Tarmo Soomere[2], Emil Stanev[1] and Jens Murawski[3]

[1] Institute for Coastal Research, HZG Geesthacht, Max-Planck-Straße 1, 21502 Geesthacht, Germany

[2] Institute of Cybernetics at Tallinn University of Technology, Akadeemia tee 21, 12618 Tallinn, Estonia

[3] Danish Meteorological Institute, Lyngbyvej 100, DK-2100, Copenhagen, Denmark

**Abstract.** Application of the preventive techniques for the optimisation of fairways in the south-western Baltic Sea and the Kattegat in terms of protection of the coastal regions against current-driven surface transport of adverse impacts released from vessels is considered. The techniques rely on the quantification of the offshore domains (the points of release of adverse impacts) in terms of their ability to serve as a source of remote, current-driven danger to the nearshore. An approximate solution to this inverse problem of current-driven transport is obtained using statistical analysis of a large pool of Lagrangian trajectories of water particles calculated based on velocity fields from the DMI/BSH cmod circulation model forced by the DMI-HIRLAM wind fields for 1990–1994. The optimum fairways are identified from the spatial distributions of the probability of hitting the coast and for the time (particle age) it takes for the pollution to reach the coast. In general, the northern side of the Darss Sill area and the western domains of the Kattegat are safer to travel. The largest variations in the patterns of safe areas and the properties of pollution beaching occur owing to the interplay of water inflow and outflow. The gain from the use of the optimum fairways is in the range of 10–30% in terms of the decrease in the probability of coastal hit within 10 days after pollution release or an increase by about 1–2 days of the time it takes for the hit to occur.

## 1. Introduction.

The increasing density of traffic and the associated increase in the pressure to the marine ecosystem is calling for new solutions for the environmental management of the potential adverse impacts. The situation is particularly complicated in areas where intense ship traffic is crossing or located near to vulnerable areas where consequences of a major accident may be extremely large (Kachel 2008). In such places it is essential to combine the rules for overall reliable design and improved safety of offshore activities, which are usually targeted to the decrease in the probability of an accident, with novel techniques of mitigation of environmental

concerns that offer ways for the reduction of the costs of an accident. The presentation of such techniques and their application to one specific ocean area with high concentration of marine traffic is the major motivation for this research.

We address in this paper the Baltic Sea which is under large pressure of shipping and other offshore activities. The number of ship operations (voyages, excluding ferry traffic) in the Baltic is estimated at 150,000 per year (Gollasch and Leppäkoski 2007), and it is assumed to considerably increase in the future. In the Baltic Sea (incl. Kattegat) about 76 ports handle more than 1 million tonnes of cargo per year. The Belt Sea and the Arkona Basin are the areas where all the ships travelling between the North Sea and the Baltic Sea have to pass through (Fig. 1) and where, thus, an optimisation of vessels' sailing line from the environmental viewpoint is an important challenge.

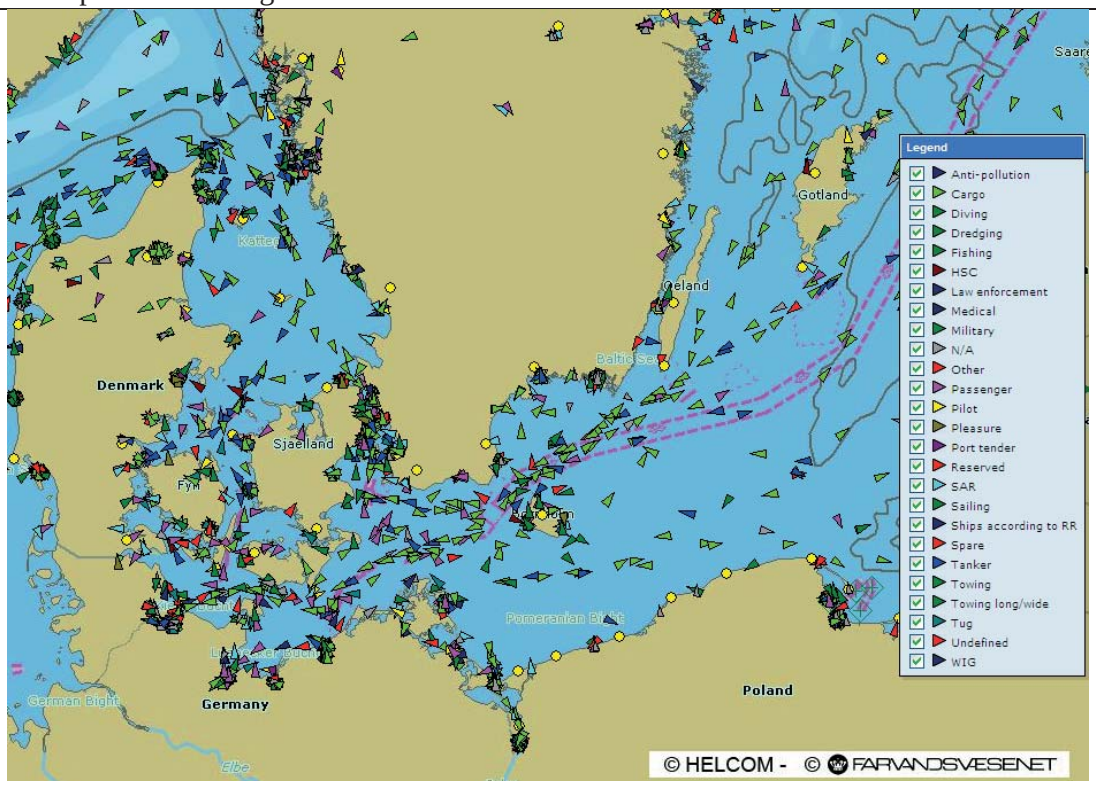


Figure 1. The ship traffic and commonly used main fairways in the western Baltic sea.

The south-western Baltic Sea is mostly shallow, with a moderate bottom slope. The key distinguishing feature of the south-western Baltic Sea is that this region serves as a transit area for the outflow of excess water through the Danish Straits. Major water exchange between the western Baltic Sea and Kattegat occurs owing to specific atmospheric conditions. The outflow is sporadically replaced by large-scale saline water inflows (Matthäus and Lass 1995). The baroclinic Rossby radius is about 5 km (Osiński et al. 2010) therefore most of medium-resolution circulation models with grid step around 2 nautical miles applied so far are barely eddy-resolving.

Furthermore fine horizontal and vertical resolution is needed to resolve straits topography and sharp stratification.

Different aspects of current-driven propagation of various adverse impacts such as oil pollution (Abascal et al. 2010), marine litter (Yoon et al. 2010), suspended matter (Gräwe and Wolff 2010) or microorganisms or toxic algae (Korajkic et al. 2009; Havens et al. 2010) have been addressed in a number of recent studies. On one hand, the exact patterns of such transport are usually extremely complicated and the beaching points of oil pollution hardly predictable in details (Vandenbulcke et al. 2009; Broström et al. 2011). On the other hand, there frequently exist semi-persistent currents and pathways of water masses at different timescales even in the sea areas where the overall dynamics is extremely irregular (Lehmann et al. 2002; Meier 2007; Soomere et al. 2011d). These pathways may support unexpectedly rapid transport of pollution in unfavourable cases. Conversely, they can be used to reduce certain adverse impacts and to implicitly protect specific regions (Soomere and Quak 2007).

In this paper we apply the techniques developed in (Soomere et al. 2010, 2011a) for the identification of environmentally safest fairways for the south-western Baltic Sea and Kattegat. The key idea is to optimise beforehand the location for the potentially dangerous activities (e.g. fairway) so that the consequences of an accident, if it happens, would be minimised. It is, for example, possible to aim at the reduction of the probability of pollution propagation from the release site to high-value regions. Equivalently, it is possible to systematically increase the time it takes for the pollution to reach such regions (Andrejev et al. 2011). The safest fairway would then go through the areas, from which the propagation of oil spills to high-value coastal areas is most unlikely. Alternatively, one could choose the fairway so that the pollution would remain offshore as long as possible. A comprehensive solution would require solving the inverse problem of pollution propagation. It is well known that inverse problems usually do not have simple solutions and, moreover, there exists no universal solution method. For this reason, statistical analysis of a large pool of particular solutions to the direct pollution propagation problem – Lagrangian trajectories of water (or tracer) particles – is employed here for the construction of an approximate solution.

The present research deals with methodological problems focussing on transport by currents, which introduces some simplifications in comparison with the real situations. Following the earlier studies, we do not account for the impact of the wind- and wave-induced drift. The reader is referred to (Ardhuin et al. 2009) for the state-of-the art of the relevant knowledge and to (Broström et al. 2011) for a recent discussion of the role of the wind- and wave-induced drift in the vicinity of our study area. Furthermore, unlike to the real pollutants, the studied here Lagrangean particles are dominated by simpler dynamics. Realistic pollutants are affected by buoyancy, vertical mixing, dispersion, spreading and other weathering processes.

We recall that the south-western Baltic Sea is shallow and weakly stratified. Weathering effects are assumed to be independent of the actual position in space and to be of minor consequence for the design study of optimum fairways. Statistical

assessments of real pollutant trajectories would reveal confidence levels to the optimum fairway designs, but would not change the designs completely. The largest difference between realistic pollutant transport and the studied current induced water particle transport is the effect of winds on the particle advection. Oil spill models add to the oil drift a fraction of 3.5% of the wind velocity in the direction of the wind (Reed et al 1994). For opposing winds and currents, and wind speeds that are one magnitude stronger than the velocity of the currents, this accounts for a decrease of 35% of the advection velocity.

Fairways in open waters are less affected by wind induced transport. Complex processes in the near coastal areas contribute to the onshore transport of particles and wave induced long-shore currents. These effects are mostly limited to the surf zone or to areas with significant gradients of wave energy: i.e. wind shadow of islands or underwater cliffs. The near coastal zone has been taken out of this study and has been replaced by a verification zone along the shoreline. Every particle that hits the zone is analysed. Therefore only offshore wave effects have been truly neglected.

Finally, we will also demonstrate that Lagrangian approach provides new insight on ocean dynamics in the transition zone, which could have useful geophysical relevance.

The structure of the paper is as follows. The circulation model and results of numerical simulations are presented in Section 2. Section 3 provides a short description of the TRACMASS code used for the calculations of Lagrangian trajectories and depicts the long-term distributions of the Lagrangian net transport speed. Section 4 provides statistics of coastal hits that serves as the basis for the choice of the parameters of Lagrangian trajectories used in the further analysis. Examples of 2D distributions of the probability for coastal hits and for the particle age are presented in Section 5 and the long-term course of integral values of these parameters is analysed in Section 6. Section 7 provides several examples of the optimum fairway.

## 2. Circulation in the western Baltic Sea, Danish straits and Kattegat

### 2.1 Numerical Model

The method for the approximate solving of the inverse problem of Lagrangian transport in the context of the identification of the optimum fairway described in detail in (Soomere 2010, 2011a, 2011b, Andrejev et al. 2011) consists of four key components: (i) a circulation model for the sea area in question, (ii) a method for the calculation of Lagrangian trajectories, (iii) a technique for the construction of the cost function that characterises the environmental risk and, finally, (iv) a procedure for the identification of the optimum location of the potentially dangerous activities. Particular realisations of the techniques may merge several steps but there is also an option to modify each step independently. This feature allows for tuning or separately

improving single steps without the loss of generality for the entire procedure (Andrejev et al. 2010; Viikmäe et al. 2010).

In this study, we use a off-line method for simulations of Lagrangian transport of selected water particles: the trajectories are calculated separately after the integration of the circulation model (Soomere et al. 2010, 2011a,b) using the TRACMASS code (Döös 1995; De Vries and Döös, 2001). The particles are locked in the uppermost layer and thus exert only horizontal advection.

The circulation model, DMI/BSH cmod, is a three-dimensional (3D) primitive equation, hydrostatic, free-surface ocean model, which has been developed originally by BSH (German Federal Maritime and Hydrographic Agency, Kleine 1994, Dick et al. 2001), further developed by DMI (Denmark's Meteorological Institute, Larsen et al.2007, Liu et al.2009, She et al. 2007) and is now known as the HIROMB-BOOS community model (Funkquist et al. 2001). It solves the Navier-Stokes equations for the currents and budget equations for temperature and salinity on a staggered Arakawa C-grid in spherical coordinates. Turbulent momentum exchange in the horizontal is parameterized following (Smagorinsky 1963) approach. A vertical mixing parameterization has been implemented based on the k-ω turbulence model that is extended for buoyancy affected geophysical flows following (Umlauf et al. 2003). The model is coupled with a sea ice model (Hibler, 1979) treating both its dynamic and thermodynamic.

In order to accurately resolve water exchange between the Baltic Sea and North Sea through the Danish Straits three nesting levels (Fig. 2a) are applied. A 2-dimensional (barotropic) NOrth Atlantic MODel (NOAMOD) with a horizontal resolution of 6 nautical miles (nm) covering a large part of the Northeastern Atlantic is used as a tool which provides boundary conditions for a Baltic Sea-North Sea model. This relatively coarse 3D model, with a horizontal resolution of 3 nm, has open boundaries between Scotland and Norway and in the English Channel. Composed tides of 14 constituents and pre-calculated surges from NOAMOD are applied to the two open model boundaries of the 3D North Sea –Baltic Sea model. Temperature and salinity at the boundaries are derived from the relevant monthly climatology and introduced into the 3D model using a sponge layer. Sea ice concentrations at the open lateral boundaries are also derived from monthly climatology.

Finally, a 3D model covering the transition area from Skagen to Bornholm (80904 surface wet points) is two-way nested (Fig. 2b) into the above Baltic Sea-North Sea model. The initial temperature and salinity data of the DMI/BSH cmod is taken from climatic data set for the Baltic Sea and North Sea.

The two-way nested grids for the North Sea – Baltic Sea (horizontal resolution of 3nm, 50 layers in the vertical) and the transition zone (0.5nm, 52 layers) have matching resolution down to 76m. The surface layer thickness is specified as 2m to account for the tidal amplitude. The layer thickness down to 30m is 2m in the North Sea – Baltic Sea model and 1m in the nested fine grid model. This high vertical

resolution enables a precise mapping of the straits and sills topography, as well as a correct representation of the thermohaline stratification. Below 30m and above 76m, both grids have the same vertical resolution of 2m. The layers below 76m are covered by the coarse grid only and feature a gradual increase in layer thickness from 2m (for all sub-surface layers above 80m) to 50m at 550m depth.

The models are driven by hourly meteorological forcing (10 m winds, 2 m air temperature, mean sea level pressure, surface humidity and cloud cover) from the DMI operational weather prediction model HIRLAM (High Resolution Limited Area Model) with a horizontal resolution of 12 km. The surface heat flux is parameterized with bulk aerodynamic formulas using atmospheric data and simulated sea surface temperature. River runoff is provided monthly for 31 rivers from the BALTEX Hydrological Data Centre (BHDC, http://www.smhi.se/sgn0102/bhdc/).

The quality and performance of the described setup of the DMI/BSH cmod circulation model has been discussed in a number of studies (see Dick et al. 2001 and Buch et al.2005). In particular, it was demonstrated that this model adequately reproduces temperature and salinity fields in the basin in question, and satisfactorily reflects the basic properties of currents in this area.

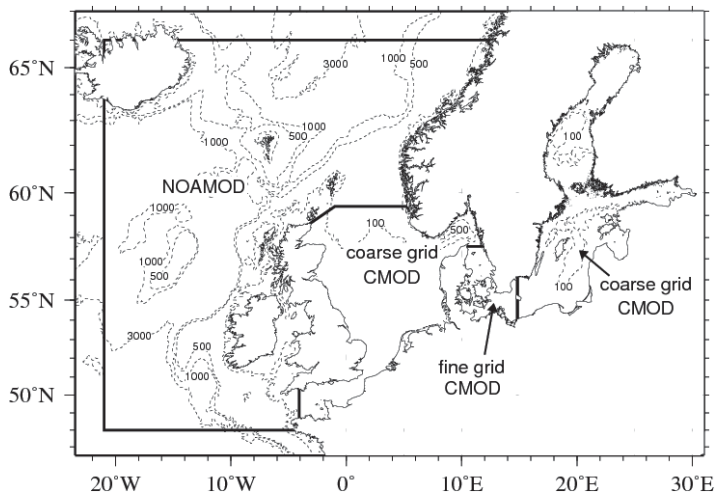


Figure 2 (a) The domains of the 2-dimensional model NOAMOD and nested DMI/BSH cmod. (b)The fine-resolution domain for the Baltic Sea-North Sea transition zone model.

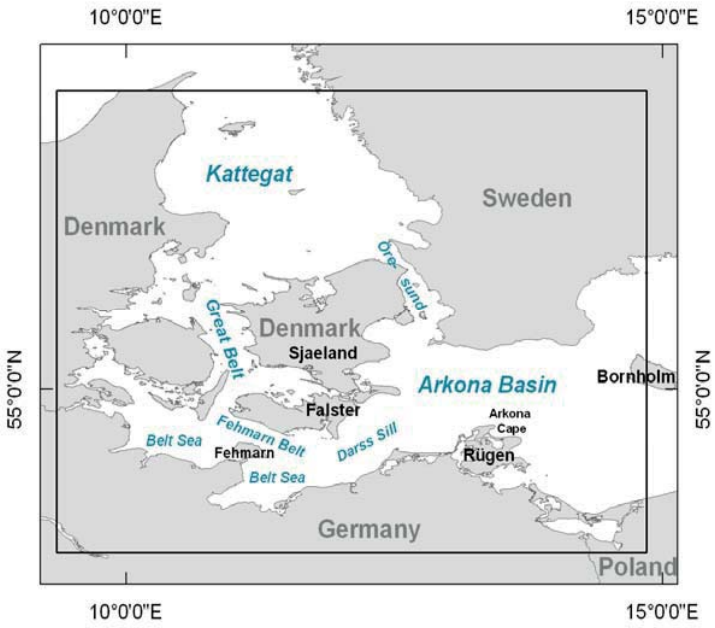


Figure 2 (b).

## 2.2 Analysis of surface transport

One of the key features controlling the flow in the transition zone is the surplus of fresh water in the entire Baltic Sea (Leppäranta and Myrberg 2009). The fresh water inflow (that is largely concentrated in areas remote from the Danish Straits) leads to a higher water level in the Baltic Sea than in the Kattegat and Skagerrak. The resulting slope supports an outflow of surface water towards the Skagerrak. This impact is clearly evident in the long-term average pattern of surface currents in the western Baltic Sea, especially for intervals dominated by the outflow situation (Fig. 3a). Note the almost total absence of persistence of currents in the Bornholm Basin and Arkona Basin and very weak average currents in the Darss Sill area (see Fig 2b). The Danish Straits show current pattern of relatively high persistence, which reflects the predomination of brackish water outflow from the Baltic Sea, channelled by the narrow straits. In the southern Kattegat, the circulation features a strong anticyclonic gyre and a relatively persistent coastal current along the western coast of Sweden.

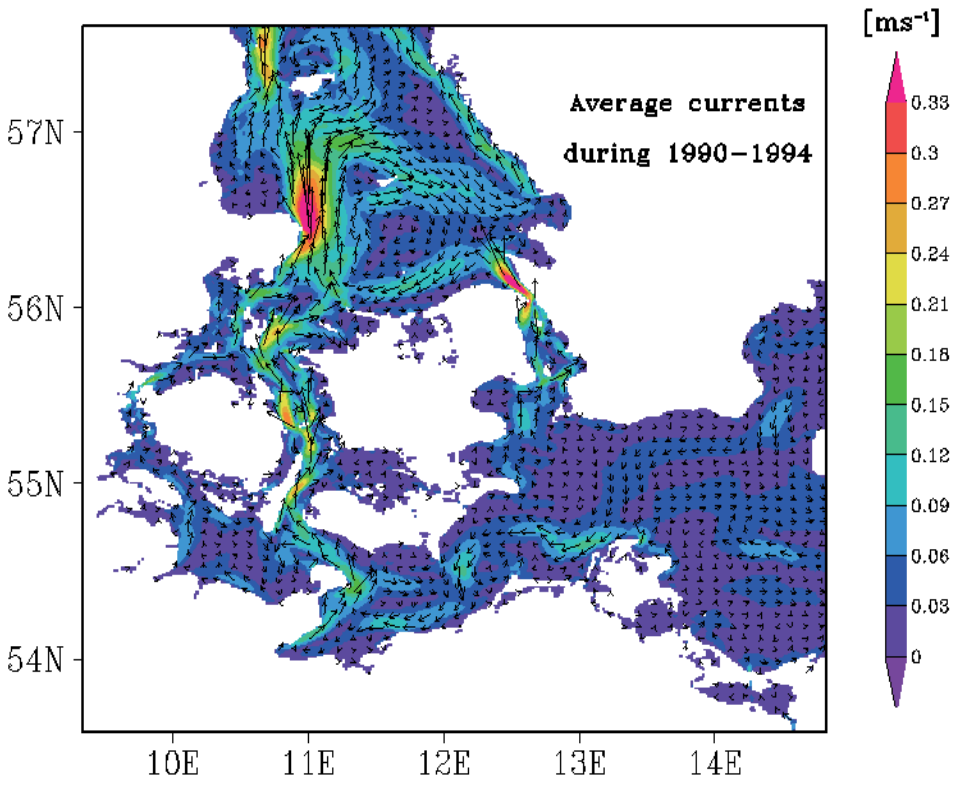


Figure 3 Five-year average surface currents in the south-western Baltic Sea, Danish Straits and Kattegat, (a) averaged for the whole period 1990–1994. (b) averaged during outflow and (c) inflow situations.

Unlike tidal estuaries, where the alternating circulation is largely dependent on tides, the alternating inflow and outflow regimes in the Baltic Sea are mainly controlled by the atmospheric forcing. We employ a simplified representation of these straits regimes based on the surface currents in the Great Belt. Situations in which the average meridional current velocity is directed to the North is assigned to the outflow and the opposite cases—to the inflow regimes. Although this simplified sorting does not necessarily reflect the presence of large-scale inflows of saline water, it makes it possible to demonstrate the difference between in/outflow current patterns.

During the typical outflow conditions (Fig. 3b) there exists a very weak structure of currents in the Bornholm Basin while an almost jet-like flow becomes evident in the Kattegat (where the anticyclonic gyre somewhat weakens) and an extremely persistent flow is present in the Straits. It is noteworthy that quite a persistent coastal surface current dominates the north-western coast of the Island of Rügen (see Fig. 2b). Further west it branches in the direction of Öresund and Great Belt. The latter branch forms two almost separated coastal currents after passing the Darss Sill.

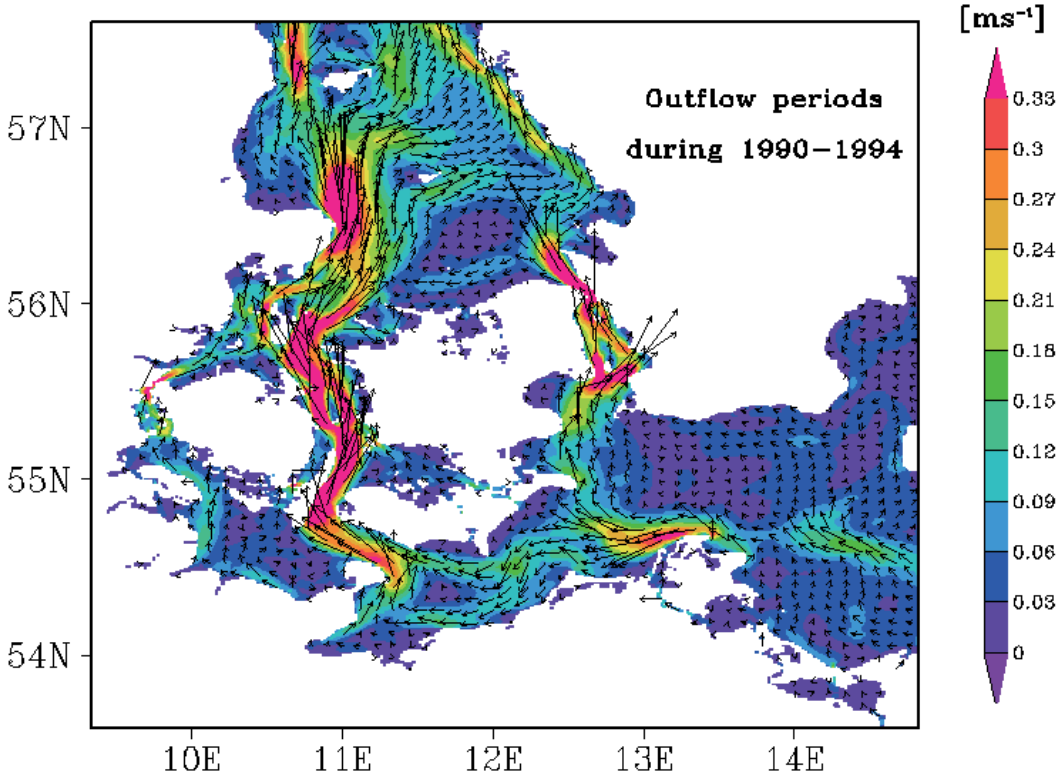


Figure 3.(b)

The circulation in the straits reverses during inflow periods (Fig. 3c). The surface waters in the Kattegat deflect to the East from the shortest way towards the Straits. Note also that during these inflow periods there exists no coastal current in the Kattegat. Instead, the Kattegat hosts an almost homogeneous surface flow to the south-east. This flow bifurcates into the Great Belt and Öresund. After passing the Straits and swells the branches merge into a coastal current near the north-western coast of the Island of Rügen. In this situation, a clearly defined jet-like flow pattern exists neither in the Kattegat nor in the Arkona Basin or Bornholm Basin.

## 3. Lagrangian trajectories and transport patterns

The second step towards an approximate solution of the inverse problem of pollution propagation is the calculation of Lagrangian trajectories of particles associated with the pollution. Following (Soomere et al. 2010, 2011a) we assume that the pollution is transported passively and thus can be associated with Lagrangian water particles. The trajectories of selected water particles are calculated after the integration of the hydrodynamic model using the TRACMASS model (Blanke and Raynard 1997; Döös 1995; De Vries and Döös 2001). This model is based on a linear

interpolation of 3D velocity fields in space and time at each point of a particular grid cell. As in the previous studies of surface pollution, we lock the trajectories in the uppermost layer (that is we deal with buoyant polluting substances).

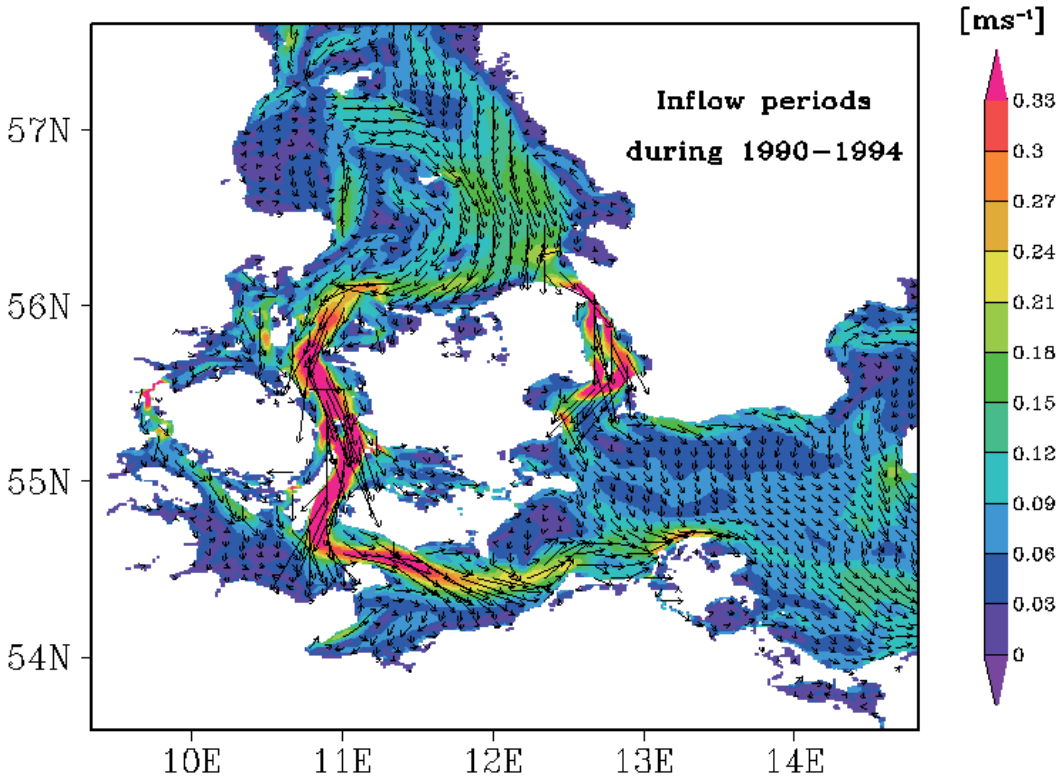


Figure 3.(c)

The applied version of the TRACMASS model ignores local spreading owing to various subgrid-scale effects such as diffusive processes, small-scale turbulence or local vertical motions of water masses. Consequently, the spreading of the trajectories is usually smaller than the spreading of real particles owing to the effect of sub-grid turbulence (Jönsson et al. 2004; Engqvist et al. 2006; Döös and Engqvist 2007; Döös et al. 2008). This means that initially close particles have an overly tendency to stay close although in the real sea they may substantially diverge. This feature is apparently not decisive for relatively short trajectories (below 10 days) but may still affect the resulting quantification of the offshore domains. As the relevant experiments towards establishing the properties of spreading in the Baltic Sea are currently in progress (K. Döös, personal communication 2011), we assume here that for the particular horizontal resolution of the ocean model and length of trajectories, ignoring of subgrid spreading does not qualitatively affect the resulting 2D fields. Notice that doing so is actually a major simplification that might not be entirely justified. There are, however, other aspects that apparently have a comparable impact

on the accuracy of the entire procedure such as the overall sensitivity of the optimum location on the resolution of the circulation model (Andrejev et al. 2011) or the choice of the measure for the environmental risks (Soomere et al., 2010; 2011c). A study of the relevant effects is, however, out of the scope of this paper.

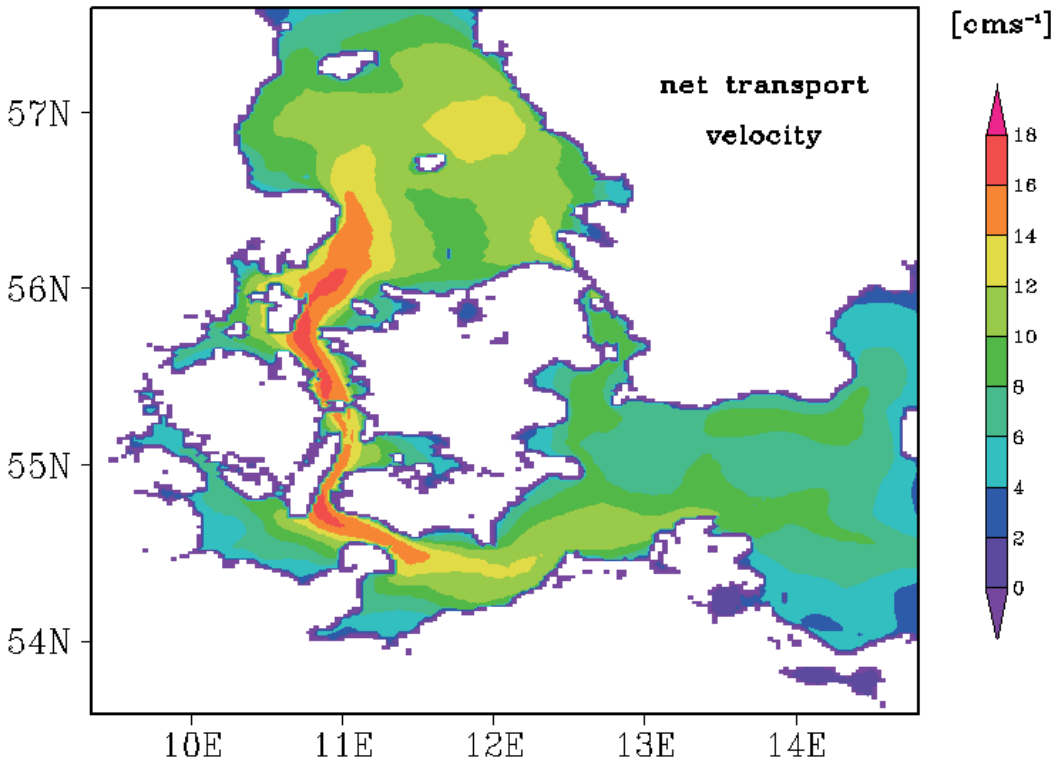


Figure 4. Average net transport velocity (cm/s) for (a) 1990–1994 and (b) 1993.

The analysis of trajectories allows the identification and visualization of several properties of surface currents that cannot be extracted directly from the current fields. The most intriguing question in terms of pollution transport is the potential presence of rapid, normally concealed, transport pathways. To a first approximation, these can be highlighted by the analysis of spatial variations in the net transport speed calculated over time windows with duration of a few days. The net transport for a water particle is defined as the distance between the start and end positions of its trajectory (Soomere et al. 2011d) and the relevant speed as the ratio of the net transport and the duration of the propagation. The procedure for the calculation of this speed follows the method proposed in (Soomere et al. 2010; Viikmäe et al. 2010). First the initial locations of 15635 water particles are specified in the innermost model area. The particles were released in each second grid cell in the east-west direction, leaving empty every second row in the north-south direction. Every target grid cell contains one particle in its centre. Their trajectories are calculated starting from 00:00 on 1 January 1990 over five days. The trajectory simulations for the same initial

positions of particles are restarted from 12:00 on 01 January for five days, at 00:00 on 02 January for five days, etc., until the end of the year 1994. Following (Soomere et al. 2010; Viikmäe et al. 2010), the time window was $t_w = 5$ days and the time lag between windows 12 hours. The net transport speed for each grid cell containing particles is estimated as an average of the relevant values for all trajectories that started from this cell at different times. In essence, a spatial pattern of the net transport speed for a particular duration of the trajectories (time window) is a natural extension of the measure of the 5-year flow persistency used in (Andrejev et al. 2004a, 2004b).

The elongated areas of the high net transport speed (Fig. 4) are the most probably candidates for rapid pollution transport pathways. The resulting map of net transport speed shows, not unexpectedly, that a fast moving and relatively persistent (at least a few days) surface flow regularly occurs in the Great Belt and directly adjacent sea areas. While such a transport is confined to the Fehmarn Belt (see Fig. 2b) by topographic reasons, its prolongation directly to the North of the Great Belt along the Danish mainland is an interesting feature of the circulation system. The long-term average net transport speed is about three times lower in the Öresund area. In essence, this feature does not necessarily reflect smaller instantaneous flow velocities and may simply signify that the flow direction changes more rapidly in Öresund than in the Great Belt. It also once more confirms that the Great Belt is the major route of water exchange during both inflow and outflow periods, and that its coasts may be impacted by pollution released far from the Straits in the Kattegat or Bornholm Basin.

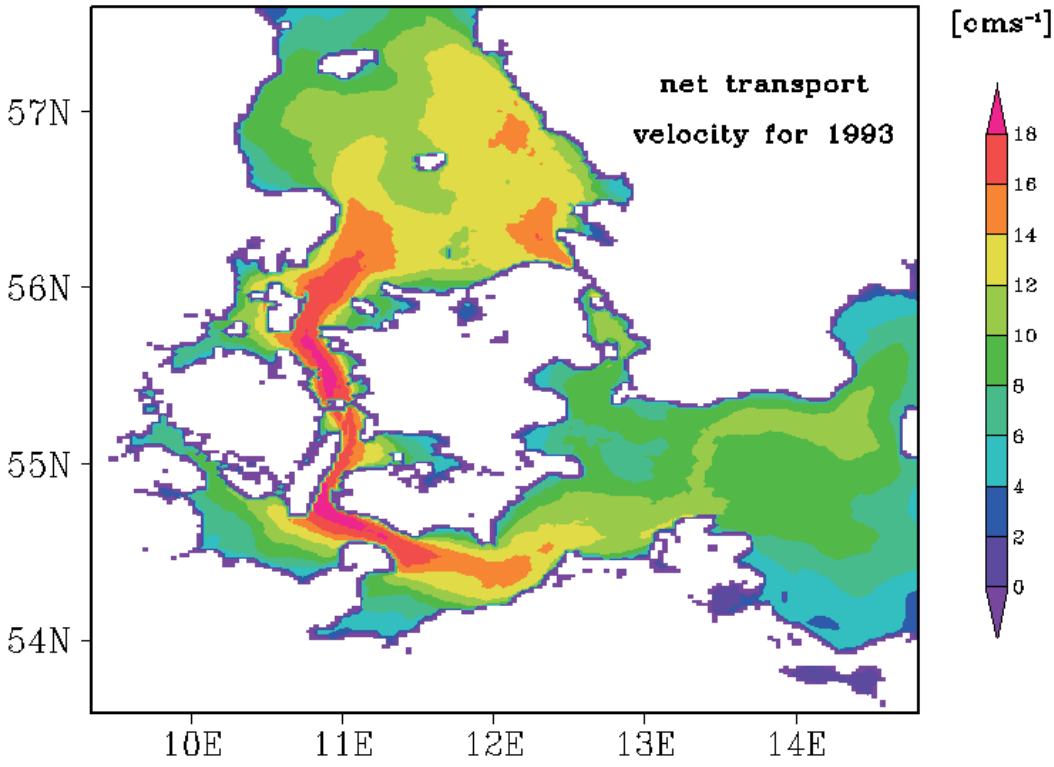


Figure 4 .(b)

There is also evidence of a wide coastal surface current along the southern coast of Sweden and to a lesser extent along the coast of Rügen (that extends to offshore to the north-east of Arkona Cape (see also Fig. 2b)). Interestingly, the coastal current along the south-western coast of Sweden, which is clearly visible in the field of average velocities, is not distinguishable in the map of net transport speed.

For further analyses the year 1993 was chosen, because of the major inflow that happened in Jannuary. The average net transport for the individual year 1993 (Fig. 4b) has a very similar pattern to that in Fig. 4a; but there is much stronger surface transport in the north-eastern part of the Kattegat near Öresund. The annual mean transport speed is almost everywhere larger than the 5-year average. Another interesting feature in the map for 1993 is the presence of a band of high net transport speed across the western Arkona Basin to the Bornholm Channel. This band signifies the possibility that pollution may relatively rapidly cross this basin under certain conditions. A similar but very weak feature is present in the 5-year average field of net transport speed.

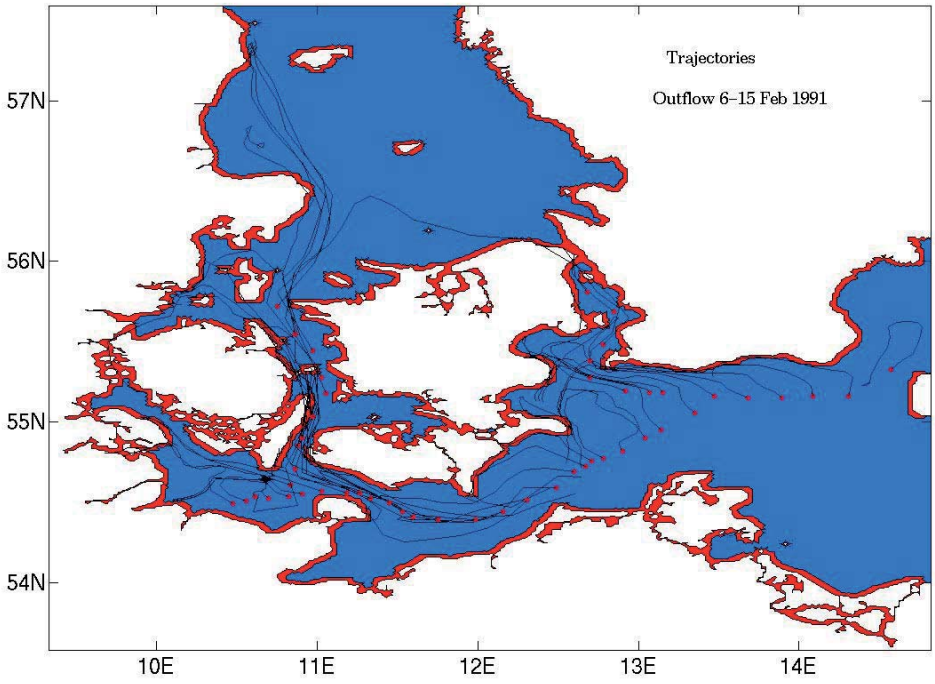


Figure 5. The trajectories of 50 particles (red circles) inserted along the major ship route (see Fig. 1) (a) at 00:00 on 6 February 1991 during typical outflow conditions (b) at 00:00 on 14 January 1993 during inflow conditions and travelling during 10 days.

## 4. Lagrangian trajectories and coastal hits

The typical appearance of Lagrangian trajectories that start from different sections of the major fairways is visualised in Fig. 5, using 50 particles distributed along the ship route. As the subsequent positions of the particles are saved after each 12 hours, the piecewise straight approximation to the trajectories may cross land areas. The above has shown that the overall flow patterns are drastically different for inflow and outflow situations. This difference becomes evident also in the behaviour of Lagrangian trajectories. Particles inserted during inflows are rapidly carried to the south along the Great Belt and Öresund, and then to the east over the Darss Sill and the Bornholm Basin. A characteristic feature, possibly corresponding to the belt of rapid net transport in Fig. 4b across the Arkona Basin, is an almost basin-scale bend of the majority of trajectories from Rügen to the north. This feature carries the particles seeded into the Great Belt and Fehmarn Belt (see Fig. 2b) region to the north until they merge with particles that started their journey from the Öresund region. This feature is not evident in long-term average patterns of the Eulerian currents (Fig. 3).

The trajectories have somewhat simpler appearance in the (more typical) outflow conditions. The particles inserted into the northern part of the Arkona Basin move to the north, some towards the Swedish coast for some time, and are then carried into Öresund. The particles that start their motion in the vicinity of the Darss Sill move more or less synchronously into the Great Belt. After passing this sound, they are carried to the North along an almost straight pathway, which matches the average Eulerian velocity field in Fig. 3 for the outflow conditions.

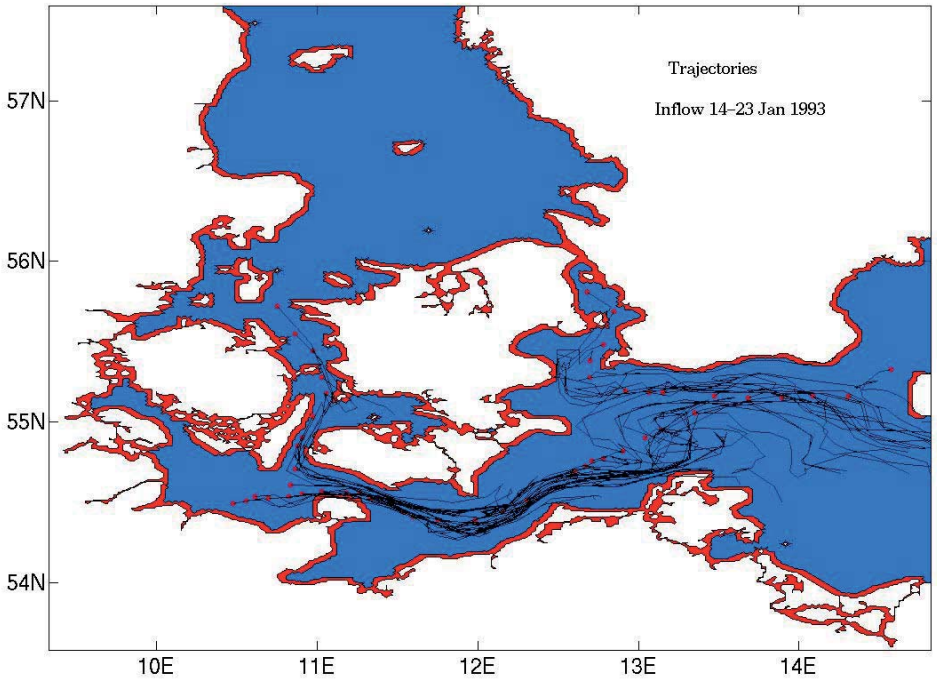


Figure 5.(b)

The presented results of simulations suggest that, during inflows, the propagation of Lagrangian particles in the Arkona Basin and in a part of the Bornholm Basin may exhibit systematic features that are not evident in the simple statistics of Eulerian currents. For outflow conditions it seems that the Eulerian current patterns reflect fairly well also the Lagrangian motions of water particles.

A more subtle difference between the inflow and outflow becomes evident in terms of the probabilities of particles to reach the costal regions, analogous to beaching of oil pollution which is called coastal hits in what follows. The used algorithm assumes that particles are allowed to drift out of the coast regions several times and to hit new coast.

For the outflow the first coastal hits occur very rapidly, within the first hours, and already on the second day almost 15% of all particles were on land (Fig. 6). This

count exceeded 20% starting from the 4th day and increased up to 36% after a week of propagation. The situation is completely different for the inflow regime. A few coastal hits in days 1–3 are exerted by particles inserted into the narrowest part of the straits. The rest of the particles are kept far from the coasts by the current system. The maximum percentage of beaching particles at any time instant only slightly exceeds 6%.

Although the drastic difference in the beaching rate in Fig. 6 is to some extent caused by inserting of the majority of the particles into the Baltic Sea, it is still evident from Fig. 5a that the tendency to rapidly hit the coasts persists for the particles that have already reached the Kattegat. The feature can be explained by the asymmetry of the hydrographic situation during the outflow and inflow. The dynamics of inflow apparently resembles to some extent the estuarine circulation forced by tidal flow. It is well known that in such cases the surface flow often exhibits a tendency to converge (Nunes and Simpson 1985). The magnitude of this effect depends on a variety of parameters of the local environment (see, e.g., Burchard et al. 2011 for detailed analysis). In simple words, the water inflowing into the Baltic Sea is usually more saline and thus more dense than the local water, and therefore exhibits a tendency to sink. Although this tendency is ignored in our simulations by locking the particles in the upper layer, the resulting 3D motion is overly convergent to the central part of the sea.

In contrast to this, the outflow conditions from the Baltic Sea are to some extent similar to what happens with ebb flow from tidal outlets or at the mouths of large rivers. The barrier effect of the (eventually tidaly-driven) salinity front (that redirects the river-laden sediment flow along the coast, Bi et al. 2010) is apparently modest in Kattegat. The divergence of the surface flow in this area is probably caused by lower salinity of the outflowing water that has a tendency to build locally higher water level and, consequently, to diverge towards the coasts.

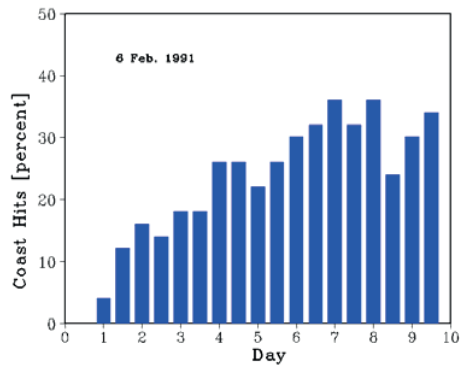


**a)**

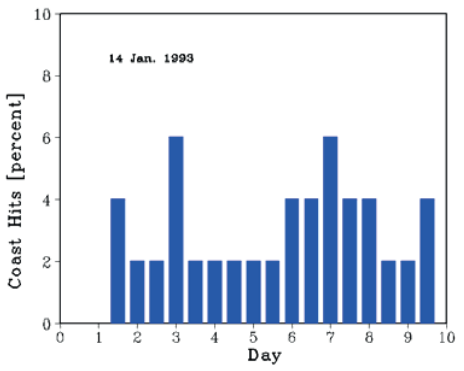


**b)**

Figure 6. Percentage of coastal hits in a particular day within 10 days of propagation for 50 particles from Fig. 5: a) for the typical outflow regime and b) inflow regime.

Such a high variability of the percentage of the coastal hits suggests that it is necessary to look at how many coastal hits occur for each time interval of simulations. As suggested in (Viikmäe et al. 2010), the optimum duration of the time window should be comparable or longer than the time during which, in average, 50% of the particles reach the coast. Figure 7 presents the average rate of coastal hits of sets of 50 particles released in locations indicated in Fig. 5 within 10 day long time windows for different release times. Different from Fig. 6, only the first hit by a single particle is counted. Typically, about 50–60% of the particles hit the coast within 10 days of propagation. This suggests that the analysis of 10–20 day long trajectories contains a sufficient amount of information (about 2200 trajectories for each grid cell, in average >1000 on them experience a coastal hit) for constructing reliable statistics.

The percentage in question varies from a level below 10% for a short period of strong inflow in mid-January 1993 up to about 95% during intense outflow periods such as around 23 February1993. Consistent with the above analysis, the deepest minima for the coastal hits are associated with saline water inflow events and the largest maxima with intense outflows.

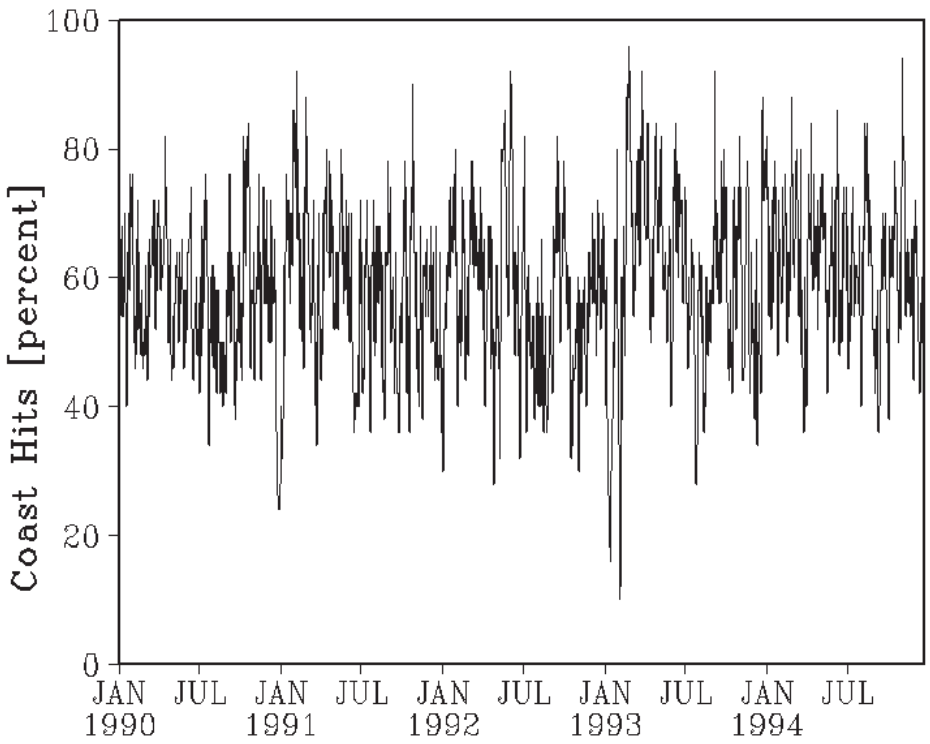


Figure 7. Percentage of particles entering the nearshore during 10 day long simulations of the drift of sets of 50 particles released in locations indicated in Fig. 5 and starting from different time instants in 1990–1994.

## 5. Distributions of the probability of coastal hit and particle age

We shall use two measures to quantify the potential of the offshore sea points to provide danger to the coast in terms of current-driven transport of adverse impacts released at a particular offshore point: (i) the average probability for a coastal hit and (ii) the average time it takes for a particle to hit the coast (called particle age in what follows) (Bolin et al. 1973; Dellhez et al. 1999; Andrejev et al. 2010; 2011). For the calculation of probabilities of coastal hits, we use the time window $t_W = 10$ days and the time lag of 5 days. The particles were released in each fourth grid cell in the east-west direction. No particles were selected from areas within 3 grid cells from the shore, as recommended in (Viikmäe et al. 2010). At each release instant, six particles were uniformly distributed in each of 3911 target cells of the innermost model domain by the TRACMASS code. This number of cells is comparable to the one used in similar calculations for the Gulf of Finland (Soomere et al. 2010; 2011c). The counter associated with each trajectory is initially set to 0 and switched to 1 if the particle hits the coast during 10 days. The relevant probability of a coastal hit for a particular grid cell and release instant is the average value of these six counters. The long-term average of this measure for each grid cell is the average over the 366 simulations extending from 01.01.1990 to the first decade of January 1995.

To calculate the particle age, one particle was selected at the centre of the set of target grid cells described above, that is, 3911 particles altogether in the model area. The time lag between time windows was also 5 days. However, in order to reach a more adequate picture of the distribution of particle age, the calculations were repeated using a time windows of 20 days. The particle age was defined as the time elapsed from the release (start of a particular time window) until the first coastal hit (Andrejev et al. 2011). It was set to 20 days if the particle remained offshore during the entire time window. The long-term average of this measure for each grid cell was also found as the average over all the relevant time windows.

The resulting maps for a single time window (Fig. 8) reveal an extremely contrast picture of probabilities, with most of the values for single cells close to 0 or 1. This high contrast is largely due to the overall tendency for the initially closely packed particles to stay together in the current version of the TRACMASS code that is visible even if only ~25% of the cells are accounted for in the calculations. The extremely large variations in the probability or age between almost neighbouring points come from the nature of the Lagrangian trajectories: when one of them touches the coast, the one that has started in the neighbourhood may not do so. In other words, frequently occurring large variations between the probabilities for neighbouring cells mostly occur because of the complexity of the geometry of the study area. This high level of contrasts and extreme gradients in maps for single time windows justifies the necessity of using as many time windows as possible in order to reach adequate climatological maps of the parameters in question.

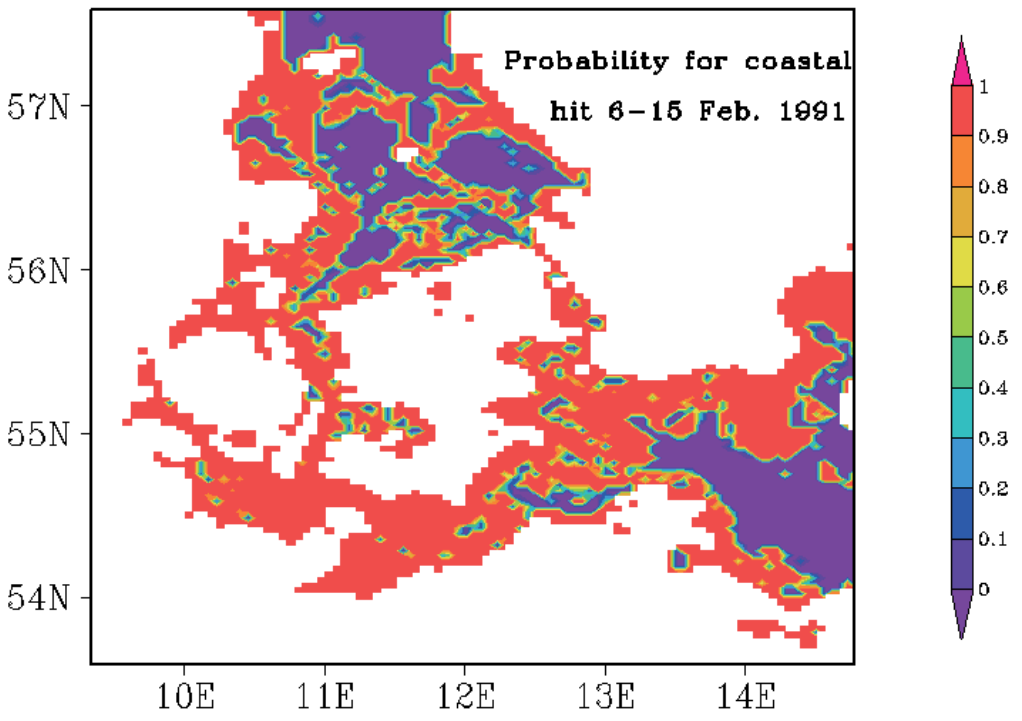


Figure 8. Probability of hitting coast for tracers released on (a) 06 February 1991 during a relatively intense outflow period (c) 14 January 1993 during an intense inflow event. Notice that the resulting values form a discrete set (0, 1/6, 1/3, 1/2, 2/3, 5/6 and 1) because of the selection procedure of particles in grid cells. Particle age (days) for tracers released on (b) 06 February 1991 during a relatively intense outflow period (d) 14 January 1993 during an intense inflow event

Leaving aside the high contrasts, maps for single time windows such as Fig. 8a still highlight several interesting features of the current-driven surface transport. On one hand, during typical outflow conditions an extensive area of low probabilities covers most of the Kattegat (Fig. 8a). Its presence apparently reflects the predomination of Lagrangian transport to the north in the surface layer and suggests that the pollution released into the Danish Straits and/or into the offshore regions of the Kattegat during these metocean conditions will be by and large transported towards Skagerrak over offshore pathways. On the other hand, the probabilities of coastal hits are very large (>0.9) in most of the Arkona Basin and in the entire domain to the south of the Danish islands. Only in certain eastern regions of the Bornholm Basin they remain relatively low.

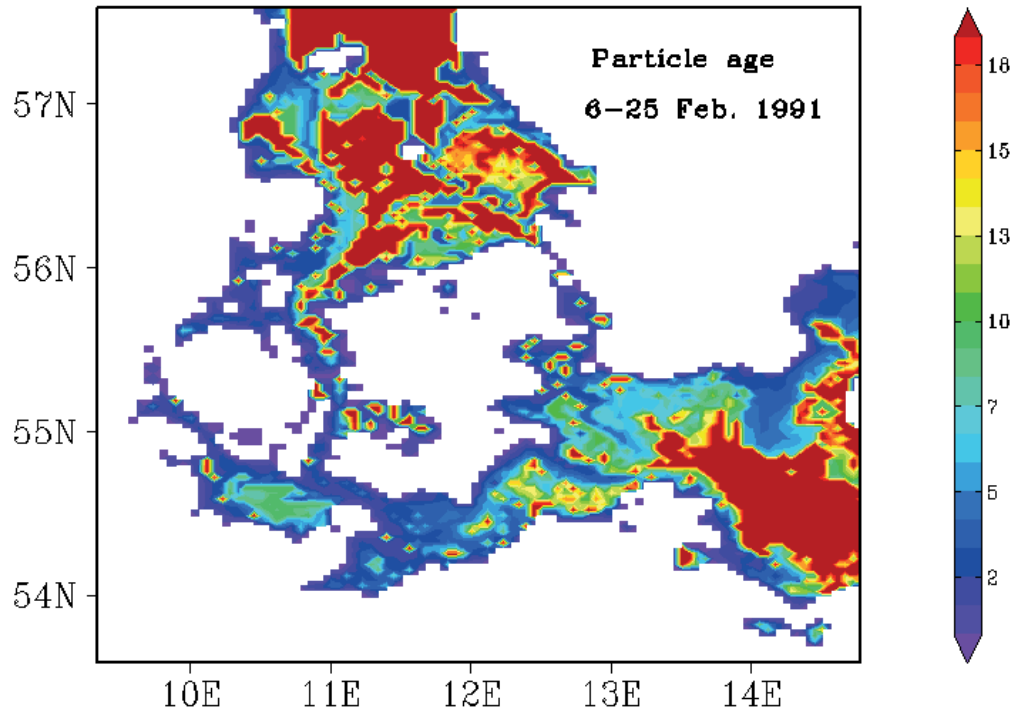


Figure 8.(b)

The spatial distribution of the particle age adds some important information to the overall high probability of coastal hits during the outflow time. Its distribution almost perfectly mirrors the distribution of the probability for the Kattegat area where it typically takes >10 days until the pollution reaches the coast. All the selected particles in the central and northern part of the Kattegat drift out of the model domain. A certain fine structure in this area in Fig. 8b evidently stems from the presence of islands. Interestingly, Fig. 8b reveals a nontrivial internal structure of current-induced drift in the Darss Sill area and to the west of Fehmarn. First of all, there is a narrow band between the Islands of Rügen and Falster (see Fig. 2b) where the particle age is by several times shorter than in the neighbouring domains. In other words, pollution released into this band has an extremely high chance to hit a coast within 1–2 days whereas similar amounts of pollution released over the Darss Sill may stay offshore for a couple of weeks. This peculiarity obviously reflects the frequent presence of an westwards-flowing current that deflects from the northern tip of Rügen and carries the surface layer to certain coastal sections (Fig. 3b). The relatively large values of particle age to the east of Fehmarn apparently stem from the low current speeds in this domain. This feature, however, may be overruled by local wind- and wave-induced drift and this area cannot be interpreted as a "safe haven".

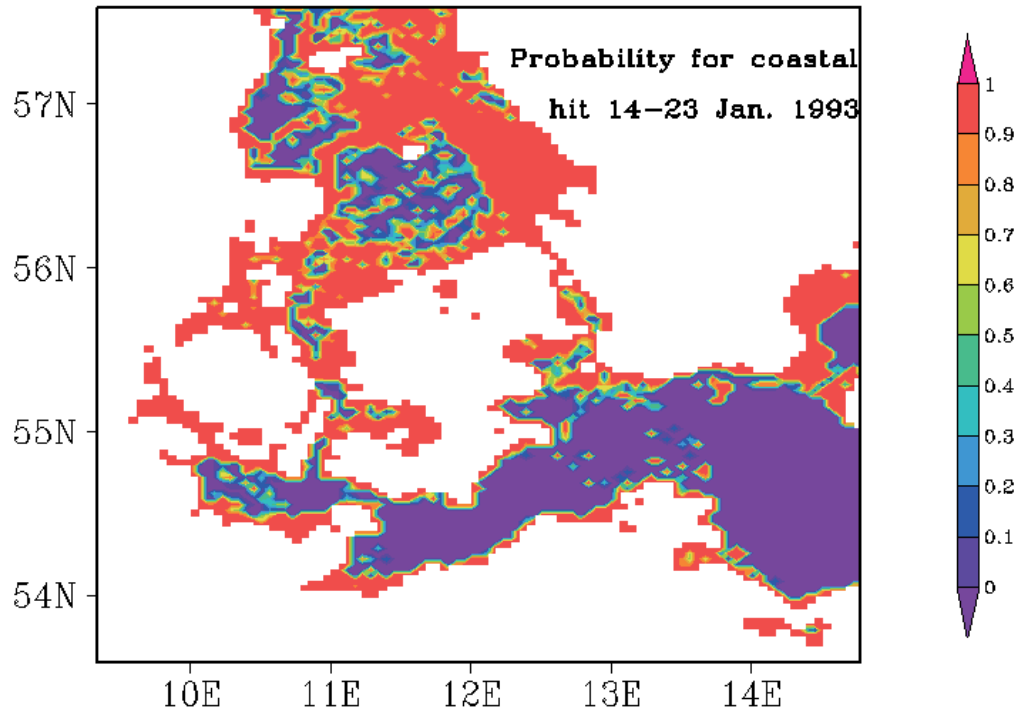


Figure 8.(c)

The situation is quite different during intense inflow events (Fig. 8c,d) when the probability for the coastal hit is very low (≤1/6) for particles released almost everywhere to the south of the Danish Straits. Accordingly, the particle age is fairly large, usually over 15 days. This feature qualitatively matches the typical pathways of tracers released along the major fairways (Fig. 5b). Surprisingly, the probability of coastal hits is equally small for the western and central areas of the Kattegat but increases considerably in its eastern domains. Similar but more detailed feature becomes evident from the distribution of the particle age (Fig. 8d). Therefore, in such metocean and inflow conditions, a considerable reduction of the probability of coastal pollution may be obtained by simply rerouting ship traffic from Öresund to the Great Belt.

To sum up, it is likely that the patterns of environmental risk associated with the events of offshore oil pollution are radically different for the typical situations of water outflow and inflow events. During the outflow periods, the pollution released in the Danish Straits and in the entire region to the south of Denmark until the Rügen-Bornholm line has a high chance to hit some coast within a few days while the pollution released in the Kattegat will either stay offshore or drift out of the region. During the inflow events, the entire south-western domain of the Baltic Sea and the

western side of the Kattegat are relatively safe whereas a pollution released in the eastern regions of the Kattegat and in the vicinity of the northern entrances to the Danish Straits has a high chance of beaching.

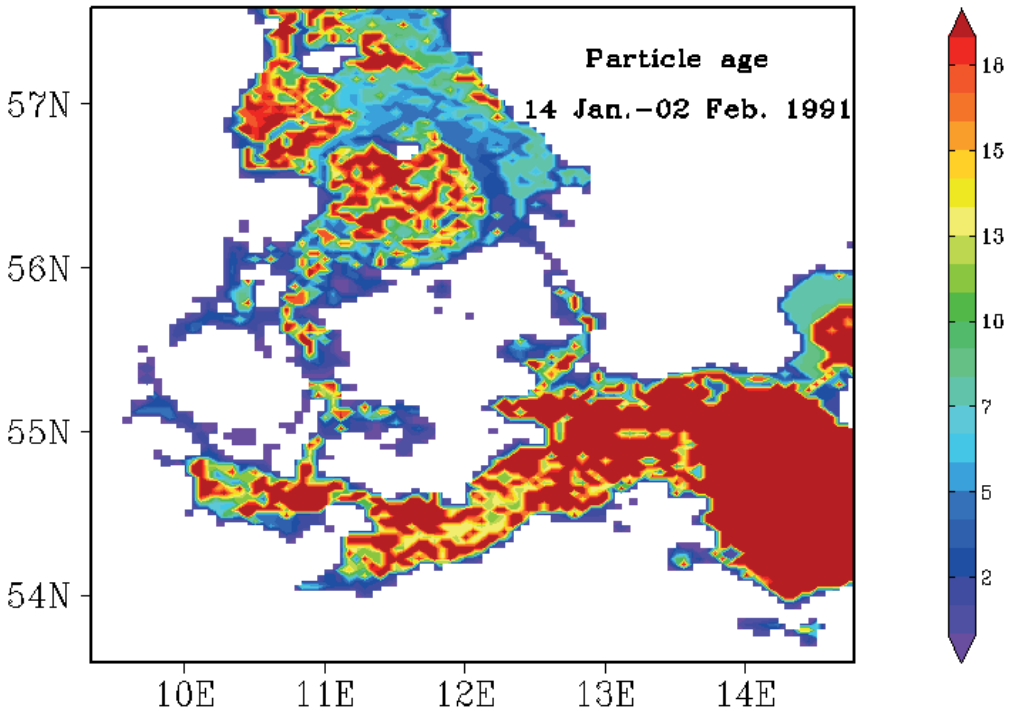


Figure 8.(d)

## 6. Long-term features of the probability of coastal hit and particle age

The similar research for the Gulf of Finland (Andrejev et al. 2011, Soomere et al. 2011c) has shown that both the 2D distributions of the probability of coastal hits and particle age as well as their integral properties for the entire sea domain in question may vary considerably with time. The variations of their average values for a single time window reveal extensive variations also in the southern Baltic Sea and in the Kattegat (Fig. 9). Interestingly, the amplitude of the variations of both quantities are almost equal for these two domains: the probability varies from about 0.1 to 0.9 and the particle age from about 5 to 27 days. In the light of the above discussion it is not unexpected that the largest variations of these characteristics are associated with strong inflow events and that the relevant values in the Baltic Sea and in the Kattegat largely mirror each other.

The temporal course of the variations in question (Fig. 9) reflects a principal difference in their basic driving factors for the Gulf of Finland and for the southern Baltic Sea. While the related environmental risks in the Gulf of Finland exhibit very

strong seasonal variation (Andrejev et al. 2011), the largest fluctuations in their values in the southern Baltic Sea are associated with the combinations of metocean conditions favourable for large-scale water inflows whereas the seasonal variations are fairly modest.

This feature explains the major reason why the cumulative values of the probability and the particle age rapidly converge to their long-term levels: about 0.5 and 11 days for the southern Baltic Sea and about 0.37 and 13 days for the Kattegat. The relatively low values of the probability (high values of the particle age) are apparently associated with the presence of open boundaries of the circulation model both in the Kattegat and at Bornholm, while the model for the Gulf of Finland has only one open boundary with the northern Baltic Proper. As the particles that drift out of the model domain are considered as safely released, a larger proportion of open boundaries naturally leads to a decrease of the estimated level of environmental risks.

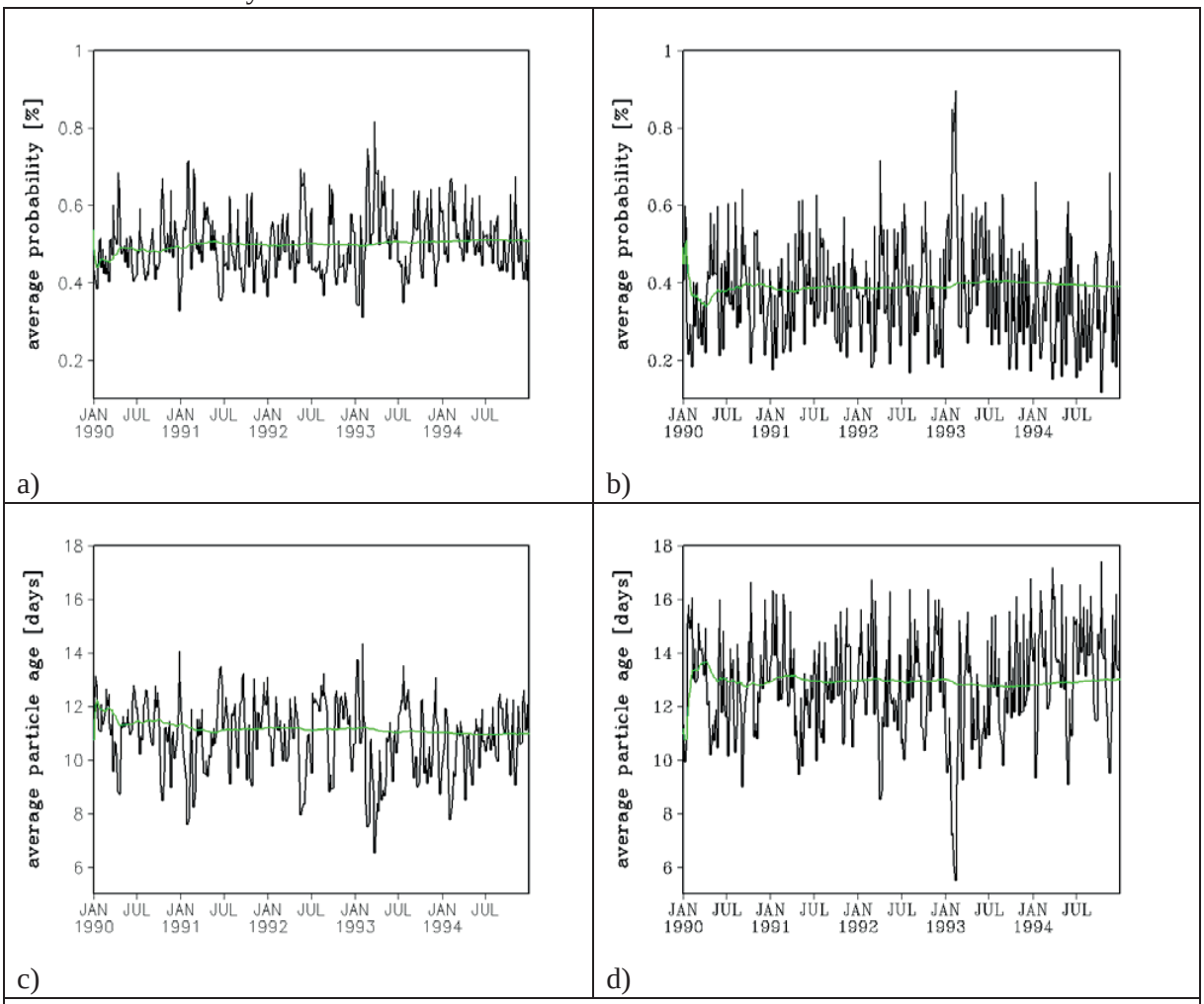


Figure 9. Mean probability (black) and cumulative averaged probability (green) for the Baltic Sea (a) (not including Kattegat) and for Kattegat (b). Mean particle age (black) and cumulative averaged particle age (green) for the Baltic Sea (not including the Kattegat) (c) and for the Kattegat (d).

It is not unexpected that several of the described features, especially the ones that correspond to inflows conditions, are averaged out in long-term distributions of the probability of coastal hits and the particle age (Fig. 10). The safest areas (in terms of both low probability for coastal hits and large particle age) are the open part of Kattegat and the sea domain to the north-east and east of Rügen.

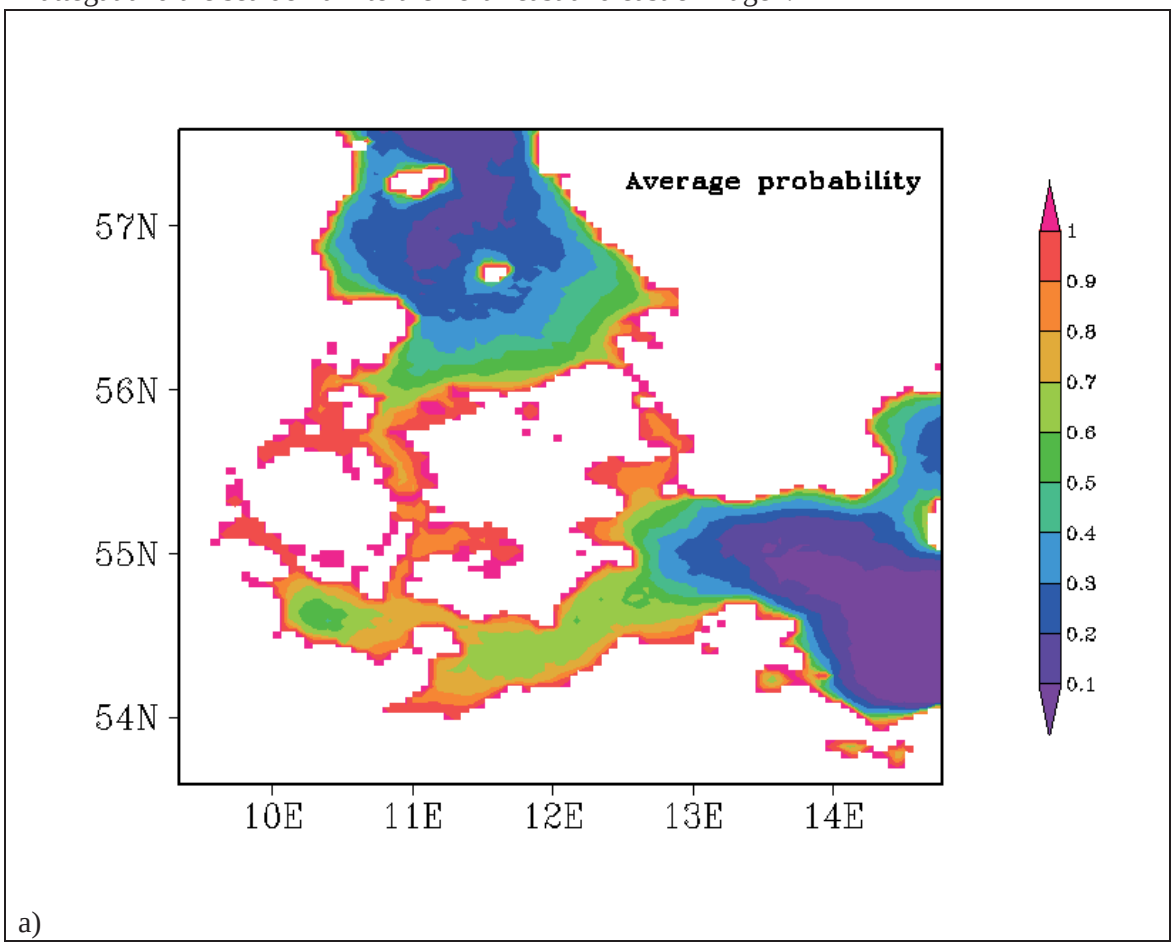


a)

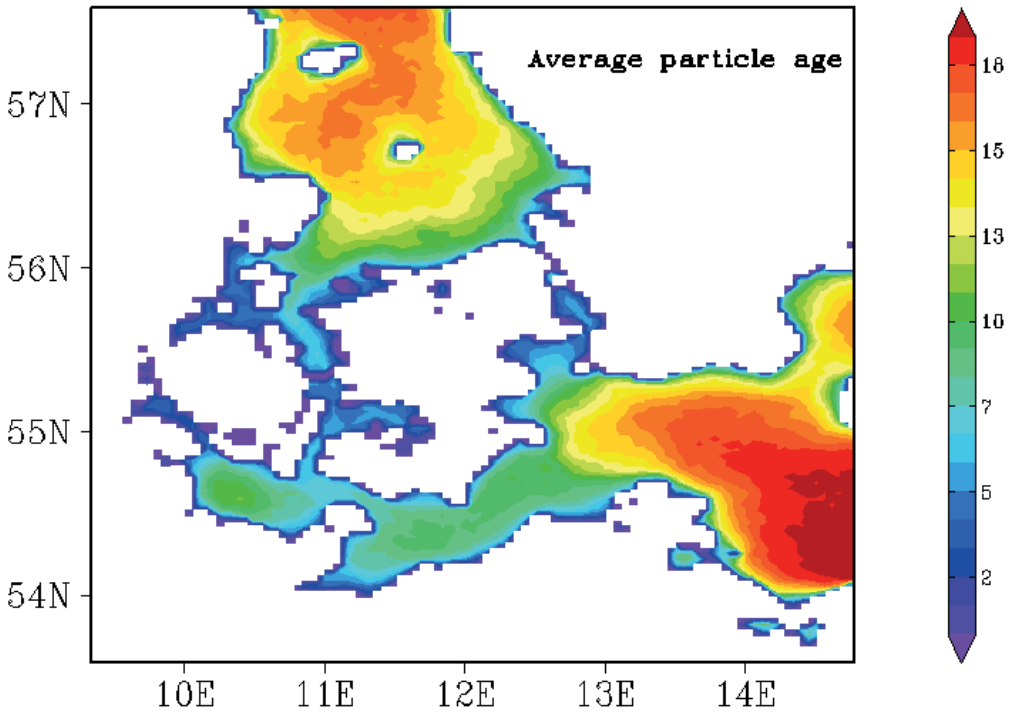


b)

Figure 10. (a) Probability of hitting a coast and (b) particle age in the western Baltic Sea for the period 1990–1994

As in similar studies of the environmental risks in the Gulf of Finland, the geometry of the safest areas does not exactly follow the geometry of the coastline. For example, the lowest probabilities and the largest particle age occur much closer to Rügen along the Bornholm-Rügen cross-section. Similarly, a relatively safe area exists in the western part of the Kattegat. A relatively safe domain to the east of Fehmarn apparently exists owing to low current velocities and simply demonstrates a rather limited ventilation rate of this region.

## 7. Optimum fairway.

Finally we consider the construction of an optimum fairway based on the calculated long-term distributions of the probabilities for coastal hits and the particle age. The traffic through the Danish Straits is confined to the existing fairways that have to follow the local bathymetry. There is more freedom in the fairway choice in the Darss Sill area and especially between Rügen and Sweden.

We employ the simple "local" method proposed in (Andrejev et al. 2010; Soomere et al. 2011b) for the selection of such fairways in elongated sea areas. The first point of the fairway is selected manually from the grid points of the circulation model either near the port of departure or at the border of a vulnerable area. The next point is sought by comparing the probabilities or particle age for the three, four or five adjacent grid points located in the general direction to the destination (Fig. 11). A natural extension of this simple scheme is to account also for the water depth and to redirect the fairway to avoid very shallow regions.

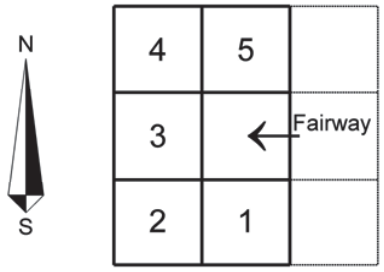


Figure 11. Scheme of the algorithm for calculating an optimum fairway heading to the west. The next fairway point is chosen from the cells of the computational grid (denoted by numbers 1–5) adjacent to the instantaneous location of the ship (marked by the arrow).

Figure 12 presents several examples of non-smoothed fairways in the model domain from the Baltic Proper to Lübeck (see Fig. 2b) based on spatial distribution of the probability for coastal hit and particle age for 1990–1994. Both the fairways from the Great Belt into Kattegat first follows the deepest channel but then deviate to the east, following the minima of the map of probabilities and the maxima for the particle age. This shape of the fairways evidently reflects the presence of an anticyclonic current system during a substantial time. This gyre keeps pollution from hitting the coast and finally transports it out of model domain. A part of the resulting fairways cross very shallow areas and cannot be used by large ships. For the practical use these "raw" estimates for the optimum fairways have to be smoothed (Andrejev et al. 2011).

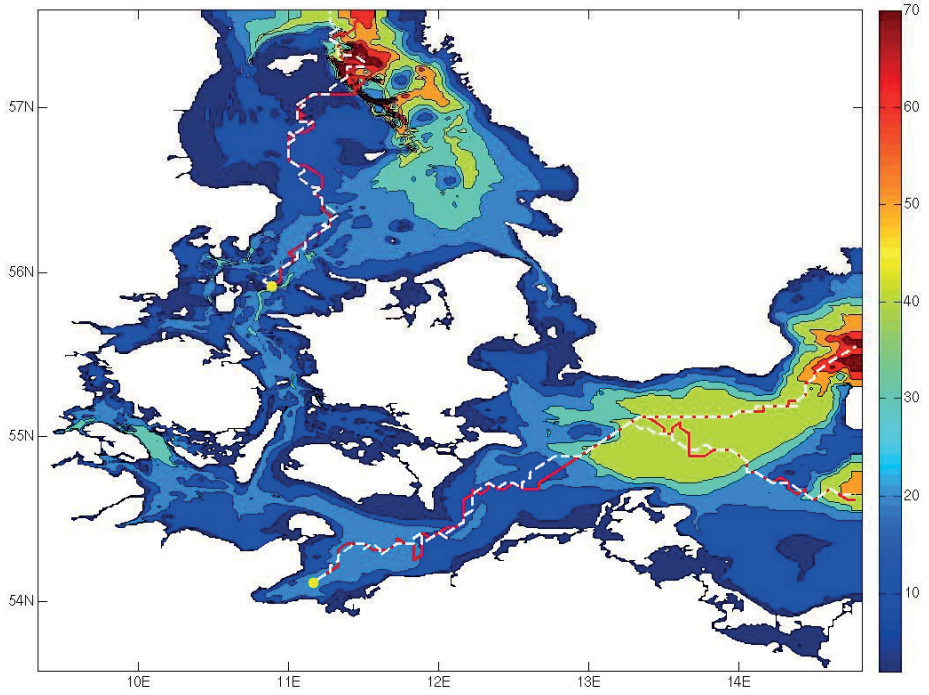


Figure 12. Optimum fairways in the western Baltic Sea based on the distribution of the probability for coastal hit (red) and particle age (white) for the period of 1990–1994. (a) Fairways starting from Lübeck and heading to the east and starting from the Great Belt and heading to the North. The yellow points indicate the starting points of the fairway and the background colour scale shows water depth (m). (b) Fairways starting from the strait between Bornholm and Swedish mainland and heading to the west and from Öresund heading to the north. (c) Fairways starting from the strait between Bornholm and Poland and heading to the west and starting from the central part of Kattegat and heading to the south. The former fairway is shifted to the south at 12.6°E, 54.7°N, after which it heads to the Belt Sea.

The fairway heading from Lübeck to the east avoids the areas in the vicinity of the Darss Sill from where the inflow current usually carries water to the coasts of Rügen (cf. Fig. 3c). The fairway corresponding to the use of the scheme in Fig. 11 with the choice from five adjacent points heads to the south-east after crossing the latitude of Arkona Cape. The branching of the fairway heading to the north-east is reached by means of restricting the sailing line from Lübeck to the east to the three neighbouring grid points located to the north, north-east and east of the current point.

Figure 12b first demonstrates that, according to the model, the optimum fairway from Öresund to the north should also go over the relatively shallow western part of Kattegat. The large fluctuations of the optimum fairway near Bornholm highlight the shortcoming of the simplest fairway finding procedure on Fig. 11 which works

properly only for elongated sea areas. The deviation of the two versions of the optimum fairway in the central Arkona basin suggest that this area has relatively low gradients of the underlying fields of probabilities and particle age and thus may serve as a natural area of reduced risk in terms of coastal pollution (Soomere et al. 2011c). As both the versions of the fairway tend to head to Öresund, they are shifted to the south by few grid points at 12.6°E, 54.7°N because we analyse the southern route. Interestingly, the fairway based on particle age heads to Lübeck while the one based on the probability of coastal hit turns to the north near Fehmarn and heads further to the Fehmarn Belt.

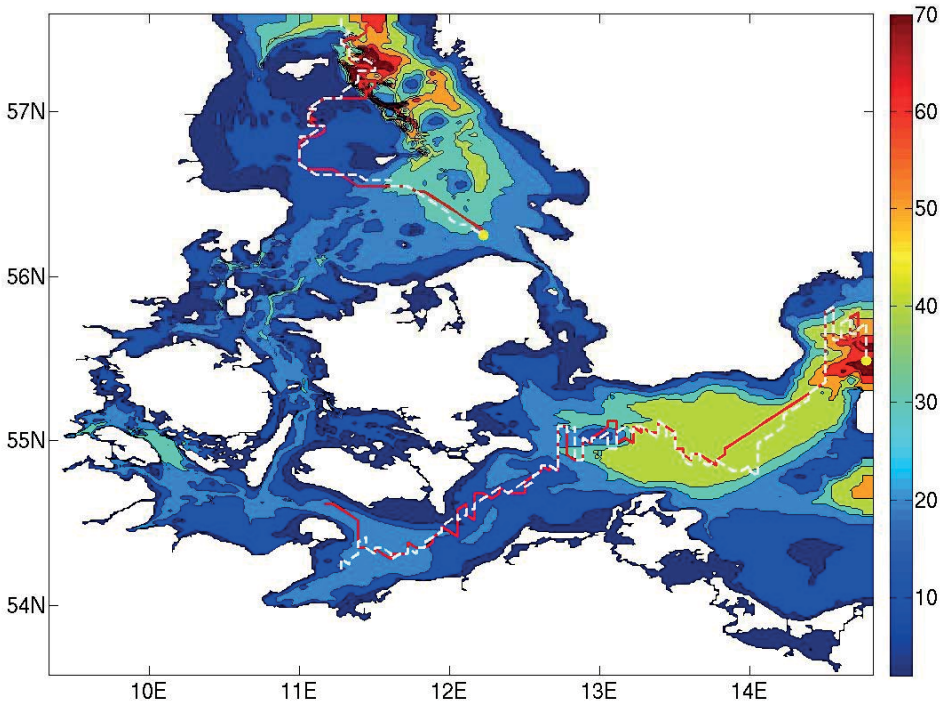


Figure 12. (b)

The gain from the use of the optimum fairways can be estimated, to a first approximation, from a comparison of the average probability of coastal hit or the particle age over the selected fairway with similar values over the commonly used fairway (Soomere et al. 2011b). A selection of results of the comparison (Table 1) shows that the benefit in terms of probabilities is modestly small for relatively safe areas such as the Kattegat but could be up to 30% for the Darss Sill area. The benefit in terms of the particle age (equivalently, in terms of extra time to combat with the pollution in the open sea) is typically about 1–2 days for the model area.

Table 1. Average particle age and probability for a coastal hit along selected optimum routes compared with the common routes extracted from Fig. 1.

| Route | Particle age, days | | Probability | |
|---|---|---|---|---|
| | Optimum | Original | Optimum | Original |
| Darss Sill–Arkona Basin | 13.3 | 10.7 | 0.37 | 0.54 |
| Darss Sill–Bornholm channel | 13.2 | 12.1 | 0.39 | 0.45 |
| Great Belt–Kattegat | 15.4 | 14.7 | 0.24 | 0.28 |
| Bornholm Channel–west | 13.8 | 12.6 | 0.39 | 0.44 |
| Sound–Kattegat | 15.7 | 14.9 | 0.22 | 0.28 |
| Arkona Basin–west | 14.7 | 12.56 | 0.31 | 0.44 |
| Kattegat-south | 14.5 | 14.25 | 0.27 | 0.29 |

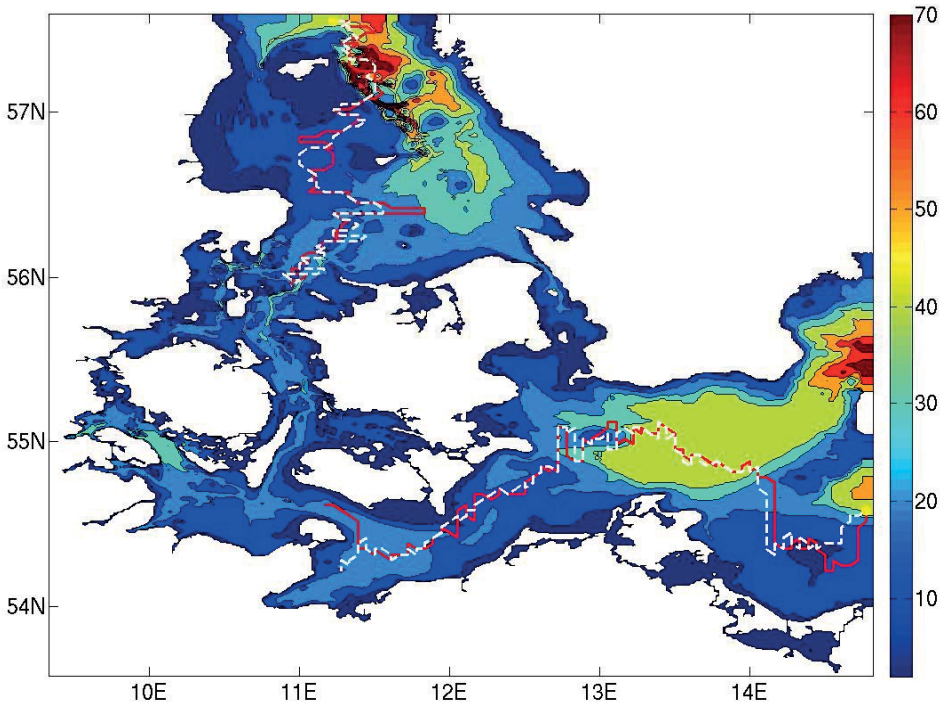


Figure 12.(c)

## Conclusions and discussion

The presented exercise uses a combination of 3D high-resolution simulations of Eulerian ocean dynamics and extensive statistical analysis of large pools of Lagrangian particle trajectories for highlighting of certain concealed features of the

current-driven transport. We can thus interpret part of the results as a new view on the circulation in the transition zone between the Baltic and North Sea. This technique makes it also possible to establish the potential of different offshore domains in terms of their "ability" to serve as sources of coastal pollution. The final step of the exercise consists in the use of the resulting distributions of probabilities for coastal hits stemming from different offshore regions and the particle age (the time it takes for the pollution to reach the coast) for estimates of the location of environmentally most safe fairways. The results are instructive in several aspects.

First of all, results revealed a major difference in the dynamics of the surface flows in the (usual) outflow conditions and in (relatively infrequent) inflow situations. There is continuously a high chance for beaching of oil spills released at basically any point of the sea during outflow time. Even those parts of adverse impacts that make their way through the Great Belt still end up at the coasts of the Kattegat with quite a high probability because of a subtle effect of flow divergence. On the contrary, the inflowing surface currents show an interesting feature of overall flow convergence towards the middle domains of the sub-basins of the south-western Baltic Sea. This convergence radically reduces the probability of coastal pollution by adverse impacts released offshore e.g. by ships. A probable physical reason for such a drastic difference in the behaviour of the surface-layer flow stems from the overall different buoyancy of the "new" surface water for the south-western Baltic Sea (where the more saline water from Kattegat tends to sink) and for the Kattegat (where the less saline Baltic Sea water tends to spread over the sea surface or to keep closer to the coasts). The resulting effects are well known for estuarine circulation (Nunes and Simpson 1985; Burchard et al. 2011) and for discharge of large rivers (Bi et al. 2010). To our knowledge, however, it has not been documented in scientific literature for Baltic Sea conditions and calls for further research in order to establish its properties and limits.

Another interesting feature of the explored region is the role of the seasonal variations. Unlike the Gulf of Finland (Andrejev et al. 2011) where the seasonal fluctuations of the forcing trigger by far the strongest signal in the variability of the probability of coastal hits and the particle age, in the studied here area the major variability of these characteristics is associated with the changes between outflow and inflow.

The narrowness of the waterways in the area in question suggests that there is very little freedom in the choice of the sailing line and thus also not very bright perspectives exist for a large gain in environmental aspects compared to wider water bodies (Soomere et al. 2011b; Viikmäe et al. 2011). Surprisingly, the spatial variations of the used measures of risk are still so substantial that even relatively small variations of the fairway under existing constraints may lead up to 30% of gain in terms of the probability of coastal pollution. The gain in terms of particle age, equivalently, additional time for removing the pollution, is relatively small but still of the order of two days.

**Acknowledgement.** This study was supported by the European Community's Seventh Framework Programme (FP/2007–2013) under Grant Agreement No. 217246 made with the joint Baltic Sea research and development programme BONUS. The research was performed within the BalticWay project, which attempts to reduce the risk of vulnerable sea areas being polluted by placing potentially dangerous activities in specific offshore regions. The research was partially supported by targeted financing from the Estonian Ministry of Education and Science (Grant No. SF0140007s11) and the Estonian Science Foundation (Grant No 7413). TS gratefully acknowledges the support of the Alexander von Humboldt Foundations for performing research in the HZG in June-September 2011.

## References

Abascal AJ, Castanedo S, Medina R, Liste M (2010) Analysis of the reliability of a statistical oil spill response model. Mar Pollut Bull 60:2099–2110

Andrejev O, Myrberg K, Alenius P, Lundberg PA (2004a) Mean circulation and water exchange in the Gulf of Finland – a study based on three-dimensional modelling. Boreal Environ Res 9:1–16

Andrejev O, Myrberg K, Lundberg PA (2004b) Age and renewal time of water masses in a semi-enclosed basin – Application to the Gulf of Finland. Tellus 56A:548–558

Andrejev O, Sokolov A, Soomere T, Värv R, Viikmäe B (2010). The use of high-resolution bathymetry for circulation modelling in the Gulf of Finland. Estonian J Eng 16:187–210

Andrejev O, Soomere T, Sokolov A, Myrberg K (2011) The role of spatial resolution of a three-dimensional hydrodynamic model for marine transport risk assessment. Oceanologia 53:309–334

Ardhuin F, Marie L, Rascle N, Forget P, Roland A (2009) Observation and estimation of Lagrangian, Stokes and Eulerian currents induced by wind and waves at the sea surface. J Phys Oceanogr 39:2820–2838

Bi NS, Yang ZS, Wang HJ, Hu BQ, Ji YJ (2010) Sediment dispersion pattern off the present Huanghe (Yellow River) subdelta and its dynamic mechanism during normal river discharge period. Estuar Coast Shelf Sci 86:352–362

Blanke B, Raynard S (1997) Kinematics of the Pacific Equatorial Undercurrent: an Eulerian and Lagangian approach from GCM results. J Phys Oceanogr 27:1038–1053

Bolin B, Rodhe H (1973) A note on the concepts of age distribution and transit time in natural reservoirs. Tellus 25:58-62.

Broström G, Carrasco A, Hole LR, Dick S, Janssen F, Mattsson J, Berger S (2011) Usefulness of high resolution coastal models for operational oil spill forecast: the Full City accident. Ocean Sci Discuss 8:1467–1504

Buch E, She J (2005) Operational Ocean Forecasting at the Danish Meteorological Institute. Environmental research, engineering and management 3(33):5-11

Burchard H, Hetland RD, Schulz E, Schuttelaars HM (2011) Drivers of residual estuarine circulation in tidally energetic estuaries: straight and irrotational channels with parabolic cross section. J Phys Oceanogr 41:548–570.

Dellhez E J M, Campin J, Hirst A C, Deleersnijder E (1999) Toward a general theory of the age in ocean modelling. Ocean Modelling 1: 17-27

De Vries P, Döös K (2001) Calculating Lagrangian trajectories using time-dependent velocity fields. J Atmos Oceanic Technol 18:1092–1101

Dick S, Kieline E, Müller-Navarra S (2001) The Operational Circulation Model of BSH (BSHcmod). Model description and validation. Berichte des Bundesatesamtes für Seeschifffahrt und Hydrographie 29/2001. Hamburg, Germany, 48 pp

Döös K (1995) Inter-ocean exchange of water masses. J Geophys Res C100:13499–13514

Döös K, Engqvist A (2007) Assessment of water exchange between a discharge region and the open sea – A comparison of different methodological concepts. Estuar Coast Shelf Sci 74:585–597

Döös K, Nycander J, Coward AC (2008) Lagrangian decomposition of the Deacon Cell. J Geophys Res C113:07028

Engqvist A, Döös K, Andrejev O (2006) Modeling water exchange and contaminant transport through a Baltic coastal region. Ambio 35:435–447

Funkquist L (2001) HIROMIB: An operational eddy-resolving model for the Baltic Sea. Bull. Maritime Inst. Gdsank 28:7-16

Gollasch S, Leppäkoski E (2007) Risk assessment and management scenarios for ballast water mediated species introduction into the Baltic Sea. Aquatic Invasions **2**: 313–340.

Gräwe U, Wolff J-O (2010) Suspended particulate matter dynamics in a particle framework. Envir Fluid Mech 10:21–39.

Havens H, Luther ME, Meyers SD, Heil CA (2010) Lagrangian particle tracking of a toxic dinoflagellate bloom within the Tampa Bay estuary. Mar Pollut Bull. 60:2233–2241.

Hibler WD (1979) A dynamic thermodynamic sea ice model. J.Phys. Oceanogr, 9: 815-846

Jönsson B, Lundberg P, Döös K (2004) Baltic sub-basin turnover times examined using the Rossby Centre Ocean Model. Ambio 23:257–260

Kachel MJ (2008) Particularly Sensitive Sea Areas. Hamburg Studies on Maritime Affairs, 13, Springer, 376 pp

Kleine E (1994) Das operatoonelle Modell des BSH feur Nordsee und Ostsee. Bundesamt fur Seeschifffart und hydrographie,126S.

Korajkic A, Badgley BD, Brownell MJ, Harwood VJ (2009) Application of microbial source tracking methods in a Gulf of Mexico field setting. J Appl Microbiol 107:1518–1527

Lasern J, Høyer J L, She J (2007) Validation of a hybrid optimal interpolation and kalman filter scheme of sea surface temperature assimilation. J. Ma. Sys. 65:122-133

Lehmann A, Krauss W, Hinrichsen H-H (2002) Effects of remote and local atmospheric forcing on circulation and upwelling in the Baltic Sea. Tellus 54A:299–316

Leppäranta M, Myrberg K (2009) Physical oceanography of the Baltic Sea, Springer Praxis, Berlin Heidelberg New York, 378 pp

Lin CH, Wu YL, Chang KH, Lai CH (2004) A method for locating influential pollution sources and estimating their contributions. Environ Model Assess 9:129–136

Liu Y, Zhu J, She J, Zhuang S, Fu W, Gao J (2009) Assimilating temperature and salinity profile observations using an anisotropic recursive filter in a coastal ocean model. Ocean Model 30: 75-87

Matthäus W, Lass HU (1995) The recent salt inflow into the Baltic Sea. J. Phys Oceanogr 25:280–286

Meier HEM (2007) Modeling the pathways and ages of inflowing salt- and freshwater in the Baltic Sea. Estuar Coast Shelf Sci 74:610–627

Nunes RA, Simpson JH (1985) Axial convergence in a well-mixed estuary. Estuar Coast Shelf Sci 20:637–649

Osiński R, Rak D, Walczowski W, Piechura J (2010) Baroclinic Rossby radius of deformation in the southern Baltic Sea. Oceanologia 52:417–429

Reed M, Turrner C, Odulo A (1994) The role of wind and emulsification in modelling oil spill and surface drifter trajectories. Spill science and Technology Bulletin 1(2):143-157

She J, Berg P, Berg J (2007) Bathymetry effects on water exchange modelling the Danish Straits. J Mar Syst 65: 450-459

Smagorinsky J (1963) General circulation experiments with the primitive equations I. The basic experiment. Mon. Wea. Rev. 91: 99-164

Soomere T, Quak E. (2007) On the potential of reducing coastal pollution by a proper choice of the fairway. J Coastal Res Special Issue 50:678–682.

Soomere T, Viikmäe B, Delpeche N, Myrberg K (2010) Towards identification of areas of reduced risk in the Gulf of Finland, the Baltic Sea. Proc Estonian Acad Sci 59:156–165

Soomere T, Andrejev O, Sokolov A, Myrberg K (2011a) The use of Lagrangian trajectories for identification the environmentally safe fairway. Mar Pollut Bull 62:1410–1420

Soomere T., Andrejev O, Sokolov A, Quak E (2011b) Management of coastal pollution by means of smart placement of human activities, J Coast Res Special Issue 64:951–955

Soomere T, Berezovski M, Quak E, Viikmäe B (2011c) Modelling environmentally friendly fairways using Lagrangian trajectories: a case study for the Gulf of Finland, the Baltic Sea. Ocean Dynamics, 62 doi: 10.1007/s10236-011-0439-y

Soomere T, Delpeche N, Viikmäe B, Quak E, Meier HEM, Döös K (2011d) Patterns of current-induced transport in the surface layer of the Gulf of Finland, Boreal Environ Res 16 (Suppl A):49–63

Stokstad E (2009) U.S. poised to adopt national ocean policy. Science 326:1618

Umlauf L, Burchard H, Hutter K (2003) Extending the $k$-$\omega$ turbulence model towards oceanic applications. Ocean Modelling 5:195–218

Vandenbulcke L, Beckers J-M, Lenartz F, Barth A, Poulain P.-M, Aidonidis M, Meyrat J, Ardhuin F, Tonani M, Fratianni C, Torrisi L, Pallela D, Chiggiato J, Tudor M, Book JW, Martin P, Peggion G, Rixen M (2009) Super-ensemble techniques: Application to surface drift prediction. Progr. Oceanogr. 82: 149–167

Viikmäe B., Soomere T, Viidebaum M, Berezovski A (2010) Temporal scales for transport patterns in the Gulf of Finland. Estonian J Eng 16:211–227

Yoon J-H, Kawano S, Igawa, S (2010) Modeling of marine litter drift and beaching in the Japan Sea. Mar Pollut Bull 60:448–463